DOI: 10.15669/pnst.5.100

Progress in Nuclear Science and Technology
Volume 5 (2018) pp. 100-103

ARTICLE

Impacts of ^{240}Pu self-shielding effect and uncertainties of σ(n,γ) at resonance energy on the reactivity controllability in HTGR inert matrix fuel

Takeshi Aoki*, Hiroshi Sagara and Chi Young Han

Tokyo Institute of Technology, 2-12-1-N1-17, Ookayama, Meguro-ku, Tokyo 152-8550, Japan

The resonance (n,γ) reaction of ^{240}Pu is one of dominant phenomena to the self-shielding effect and the reactivity controllability in plutonium fuel for high temperature gas cooled reactors (HTGRs) aiming to deep-burning. Impacts of the mitigation of the self-shielding effect and nuclear data uncertainties for the resonance (n,γ) reaction of ^{240}Pu on the reactivity controllability were investigated for various fuel design using MVP code. k_∞ decreased from 1.3 to 1.05 and reactivity fluctuation decreased from 30% to 6% in the proposed inert matrix fuel (IMF) design with a dilution of the TRU oxide kernel and the neutron spectrum control because of mitigation of ^{240}Pu self-shielding effect at 1.056-eV.

Keywords: TRISO; HTGR; plutonium; deep burn; self-shielding effect; MVP

1. Introduction

The utilization and transmutation of the transuranic (TRU) nuclides in the form of ceramic-coated fuel particles through a high burnup irradiation (Deep burn) has been studied in high temperature gas cooled reactors (HTGRs) to reduce a volume of high level radioactive waste [1-4]. In the study on deep-burning, utilization of inert matrix fuel (IMF) which is TRU oxide diluted with neutronically inert matrix has been proposed for low initial excess reactivity and higher fuel burn-up by reducing self-shielding effect of ^{240}Pu [3-5]. Especially, a significant resonance capture cross section (σ(n,γ)) at 1.056-eV of ^{240}Pu contributes to the self-shielding effect. The nuclear data uncertainty in the reaction of ^{240}Pu is about 5% for low incident neutron energy and higher relative to other major reaction such as about 1% for ^{239}Pu fission reaction and about 0.5% for ^{235}U fission reaction. Therefore, the nuclear data uncertainty can cause much uncertainty in reactivity evaluations than conventional fuel.

In the present paper, impacts of the self-shielding effect and nuclear data uncertainty of ^{240}Pu capture cross sections on the initial reactivity and reactivity fluctuation are studied.

2. Calculation method and model

In this study, the core model used is the Clean Burn reactor which is specifically designed with the aim of rapid Pu incineration. The Clean Burn reactor is a prismatic block type HTGR developed by Japan Atomic Energy Agency (JAEA) based on GTHTR300 [5]. The number of fuel columns is 144 in the core. Each fuel column is composed of 8 fuel blocks, which have a height of approximately 1 m in the axial direction. The fuel block geometry is referred to the literature. The fuel block has 57 coolant holes in which fuel rods including 70 fuel compacts are inserted. **Figure 1(a)** shows the calculation model based on a two-dimensional infinite body, which is created from the fuel block to simulate equivalent incineration features. Each fuel compact is composed of a graphite matrix and many tristructural isotropic (TRISO) fuel particles randomly dispersed in the graphite matrix. The TRISO fuel particle, composed of a fuel kernel and four carbide layers, is a small particle of less than 1 mm in diameter, as shown in **Figure 1(b)**.

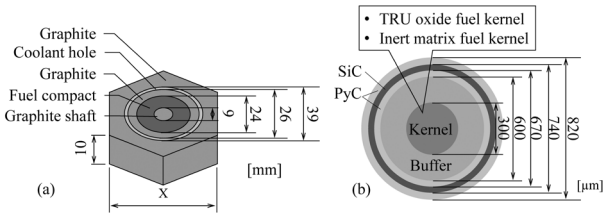

Figure 1. Geometry of calculation models: (a) two dimensional infinite body and (b) cross section of the TRISO fuel particle.

The neutron transport and burnup calculations are conducted using the Monte Carlo neutron transport code MVP/GMVP version II and evaluated nuclear data library of JENDL-4.0 [6,7]. Moreover, a statistical geometry model is also employed to treat the double heterogeneity effect created by the multi-coated fuel

*Corresponding author. Email: aoki.t.am@m.titech.ac.jp

particle [8]. The pitch of the fuel compacts and the fuel kernel composition are considered as parameters. The packing fraction of TRISO fuel particles in the fuel compact is changed, keeping the amount of the nuclear material constant; to model current engineering limitations, the packing fraction is assumed to be lower than 35 vol.% to maintain the integrity of TRISO fuel particles in the fuel fabrication process [9]. The TRU oxide (TRUOx) fuel kernel and IMF kernel, which is a homogeneous solid solution of TRUOx and yttria stabilized zirconia (YSZ) are modeled as fuel kernels. The composition of TRU used in this study is shown in **Table 1**, based on TRU, excluding curium, recycled from typical light water reactor (LWR) spent fuel without cooling. The YSZ is modeled as a homogeneous solid solution of ZrO_2 and $YO_{1.5}$. The ratio of ZrO_2 and $YO_{1.5}$ is assumed to be 78.9:21.1 mol.%. The core configurations and the specifications of each component used for the calculation are shown in Table 1.

Table 1. Core configuration and specifications of each component.

Core configuration		
Heavy metal inventory [t]		1.26
Liner power density [MW/cm]		8.70E-05
Core height [cm]		840
Number of fuel block in a layer		144
Fuel block		
Number of fuel rods in a fuel block		57
Pitch of the fuel block [cm]		33.9
Height of the fuel block [cm]		105
Density of the fuel block without fuel rods [g/cm^3]		1.74
Diameter of coolant hole [cm]		3.9
Fuel rod		
Length of the fuel rod [cm]		105
Outer diameter of the fuel rod [cm]		2.6
Inner diameter [cm]		2.4
Number of fuel compacts in a fuel rod		70
Density of the fuel rod without fuel compacts (graphite) [g/cm^3]		1.74
Fuel compact		
Inner diameter [cm]		0.9
Outer diameter [cm]		2.4
Length [cm]		1.5
Density of graphite matrix and graphite shaft [g/cm^3]		1.74
Multi coated fuel particle		
Kernel	Thickness [μm]	150
	Density [g/cm^3]*1	-
Buffer	Thickness [μm]	150
	Density [g/cm^3]	1
Inner pyrocarbon	Thickness [μm]	35
	Density [g/cm^3]	1.87
Silicon carbide (SiC)	Thickness [μm]	35
	Density [g/cm^3]	3.2
Outer pyrocarbon	Thickness [μm]	40
	Density [g/cm^3]	1.87

*1 It is calculated based on the density of PuO_2 (11.46 [g/cm^3]) and its atomic density was conserved in any compositions.

3. Impacts of the self-shielding effect on the reactivity

3.1. Impacts of nuclear fuel dilution

The neutron transport and burnup calculation model used a fuel compact pitch of 6.1 cm and TRUOx fuel kernels. As shown in **Figure 2**, the high resonance σ(n,γ) of ^{240}Pu at 1.056-eV (~10^5) caused a significant neutron flux depression in the vicinity of the resonance. This phenomenon is referred to as the energy self-shielding effect. These self-shielding effects reduce the neutron capture reaction rate of ^{240}Pu and ^{241}Pu production in the fuel kernel. The following equation shows that the energy and spatial self-shielding effects can be mitigated by the dilution of the fuel kernel [10]:

$$\phi^E = \frac{\Sigma_s^M}{\left[\Sigma_t^E - \Sigma_s^{E,A}\right]E} \approx \frac{\sigma_b}{\left(\sigma_b + \sigma_a^E\right)E} \quad (1)$$

In Eq. (1), ϕ is the neutron flux, Σ_t and Σ_s are total and scattering reaction rates, respectively, and σ_b and σ_a are background and absorption cross sections, respectively. The superscript M represents moderator and E is energy group. If the background cross section of the moderator is increased by diluting the fuel kernel with inert matrix, the neutron flux and capture reaction rate of ^{240}Pu is expected to recover.

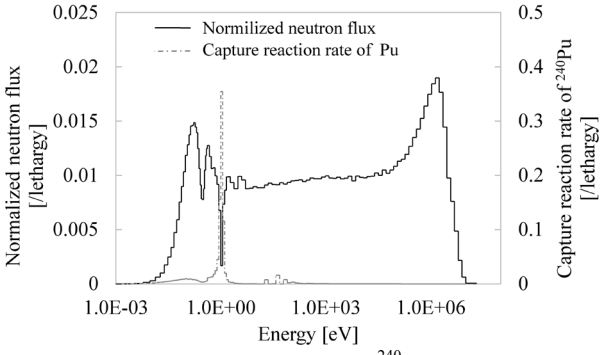

Figure 2. The self-shielding effect of ^{240}Pu in $TRUO_X$ kernel.

The effect of the dilution of the fuel kernel on incineration features was studied, maintaining the fuel compact pitch of 6.1 cm. **Figure 3** shows the k_∞ variations with burnup for five different compositions of IMF: TRUOx:YSZ = 100:0; 90:10; 77:23; 60:40; and 49:51 wt.%. Higher dilution rates resulted in lower initial excess reactivity, smaller burnup reactivity fluctuation, and higher burnup indicating that this mitigation of the self-shielding effect of ^{240}Pu increased the neutron capture reaction rate of ^{240}Pu and the ^{241}Pu production. The excess reactivity will be managed by negative reactivity insertion with control rod. Less initial excess reactivity and burnup reactivity fluctuation can be easily and efficiently controlled with the control rods. This study showed that the IMF design with TRUOx:YSZ = 49:51 wt.% could achieved better reactivity controllability and higher burn-up.

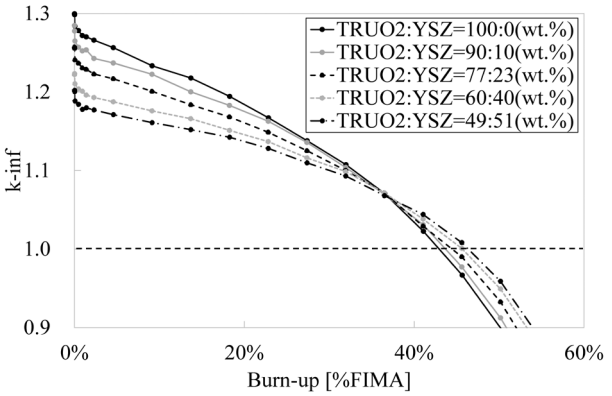

Figure 3. Variation in k_∞ relative to burnup for IMF kernels with different compositions.

3.2. Impacts of neutron spectrum hardening

The neutron spectrum controls the absorption reaction rate and the neutron flux in the resonance region. Based on this relationship, it is possible to increase the neutron capture reaction rate of ^{240}Pu by adjusting the neutron spectrum. The impact of the neutron spectrum on reactivity is investigated for the IMF kernel consisting of TRUOx:YSZ = 49:51 wt.%. **Figure 4** shows the k_∞ curves in the calculation model for fuel compact pitches of 6.1, 5.6, 5.1, 4.6, and 4.1 cm. The neutron spectra hardened with lower ratios of moderator to fuel volume because of the reduction of the fuel compact pitch. The small fuel compact pitches resulted in lower initial excess reactivity and higher maximum burnup because the harder neutron spectra inhibited the fission reaction of ^{239}Pu at the beginning of burnup and increased ^{241}Pu production at the epithermal region. However, to attain criticality during the operation, the k_∞ must exceed one. The IMF kernel with a fuel compact pitch of 5.1 cm (referred as Opt. IMF kernel) yielded the best reactivity controllability in terms of low initial excess reactivity and little fluctuation in burnup reactivity. The initial excess k_∞ improved from approximately 0.3 to 0.06, compared to the TRUOx kernel. The burnup reactivity fluctuation, defined as the ratio of the difference between maximum and minimum k_∞ to minimum k_∞, also improved from approximately 30% to 6%.

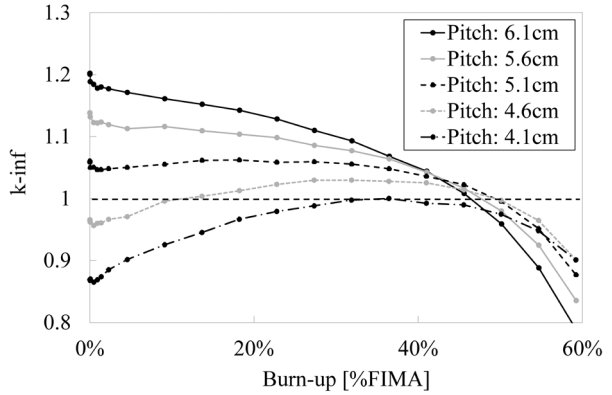

Figure 4. Variation in k_∞ relative to burnup for IMF kernels with different fuel compact pitches. (TRU:YSZ = 49:51 wt.%)

3.3. Impacts of the self-shielding effect

Figure 5 shows the variation in the relative neutron capture reaction rates of ^{240}Pu for different depths to the peak at surface of kernel in (a) the TRUOx kernel and (b) the optimized IMF kernel and fuel block, in which TRUOx:YSZ = 49:51 wt.% and the pitch is 5.1 cm. Comparing Figure 5(a) and Figure 5(b) shows the sharp decrease in the macroscopic capture reaction rate at resonance regions in the inner layer of the IMF kernel caused by the spatial self-shielding effect; remarkably, this decrease is recovered, especially in the vicinity of the resonance. Therefore, the mitigation of the self-shielding effect promoted ^{240}Pu capture reaction rate and ^{241}Pu production in the optimized IMF kernel to a greater extent than in the TRUOx kernel.

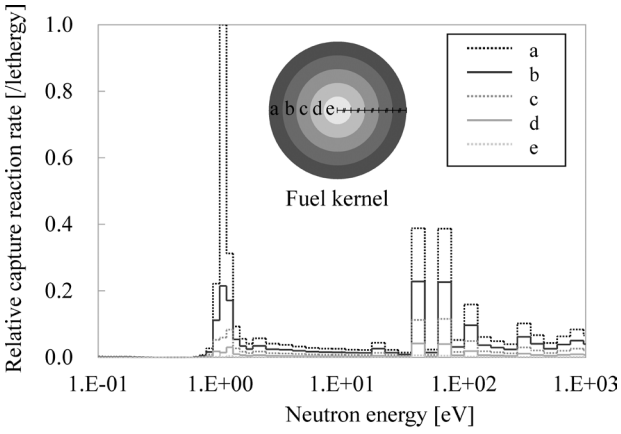

(a) TRUOx kernel

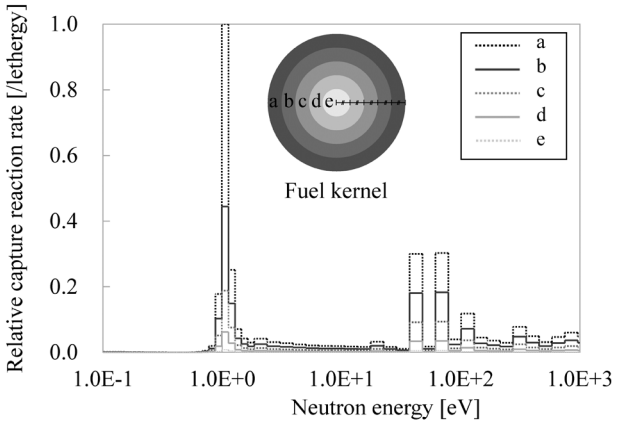

(b) IMF kernel

Figure 5. Variation in neutron capture reaction rates for different depths in (a) TRUOx and (b) IMF kernels.

3.4. Impacts of the nuclear data uncertainty

Uncertainty in ^{240}Pu $\sigma(n,\gamma)$ at resonance energy is one of dominant factor to the feasibility of the reactivity control. Uncertainties in k_∞ were evaluated propagating the relative uncertainties for σ_c and σ_f in JENDL4.0. The relative uncertainty in k_∞ is assumed to be proportional to the relative uncertainty in neutron reproduction rate (η) which represents the number of fission neutrons that result per absorbed neutron in the fissile isotope defined

in following equation.

$$\eta = \frac{\sum_i \sum_E \nu_c^{i,E} \sigma_f^{i,E} \phi^{i,E} N^i}{\sum_i \sum_E \{\sigma_c^{i,E} + \sigma_f^{i,E}\} \phi^{i,E} N^i} \quad (2)$$

The relative uncertainty in η and effective cross section of reaction n for nuclide i (σ_n^i) are calculated by the error propagation equation and the error-weighted average, respectively.

$$Err(k_\infty) = Err(\eta) = \sqrt{\sum_i \left[\left\{ \frac{\partial \eta}{\partial \sigma_f^i} \Delta \sigma_f^i \right\}^2 + \left\{ \frac{\partial \eta}{\partial \sigma_c^i} \Delta \sigma_c^i \right\}^2 \right]} \quad (3)$$

$$Err(\sigma_n^i) = \frac{\Delta \sigma_n^i}{\sigma_n^i} = \frac{\sum_E \{\sigma_n^{i,E} \phi_n^{i,E} N^i \times Err(\sigma_n^{i,E})\}}{\sum_E \{\sigma_n^{i,E} \phi_n^{i,E} N^i\}} (n = c, f) \quad (4)$$

where Err(X) is relative uncertainty in X, ΔX is absolute uncertainty in X, N is atomic number, ν is averaged neutron production per a fission reaction, σ_f and σ_c are the fission and capture cross sections, respectively. Superscripts i is representing nuclides.

The k_∞ and evaluated uncertainties for 0, 41 and 55%FIMA are summarized in **Table 2**. The uncertainties in k_∞ increased from 1.3% in the TRU oxide fuel kernel to 1.8% in the IMF kernel at 0%FIMA due to more significant contribution of uncertainty in ^{240}Pu resonance σ(n,γ) at 1.056eV to the propagated uncertainty in k_∞. Even Opt. IMF kernel, k_∞ at 0%FIMA was larger than one to achieve criticality considering nuclear data uncertainty. Therefore, results revealed that the proposed fuel design was able to exceed k_∞=1 at initial burn-up, attain criticality and initiate the reactor. For irradiated fuel, contributions of nuclear data uncertainties of fission products and fission yields have to be evaluated to discuss the feasibility of the reactor.

Table 2. k_∞ with uncertainty for various burn-up.

Kernel	0%FIMA	41%FIMA	55%FIMA
TRUOx	1.3±0.017	1.02±0.014	0.82±0.015
IMF	1.2±0.018	1.04±0.019	0.89±0.016
Opt. IMF	1.06±0.019	1.04±0.017	0.95±0.016

4. Conclusion

Impacts of the mitigation of the self-shielding effect and nuclear data uncertainties for the resonance capture reaction of ^{240}Pu on the reactivity controllability were investigated for various designs of inert matrix fuel in high temperature gas cooled reactors (HTGRs).

Calculations based on the carbide fuel compact cell revealed that the initial infinite multiplication factor decreased from 1.3 to 1.06 in the proposed inert matrix fuel (IMF) design with a dilution of the TRU oxide kernel and the neutron spectrum control because of mitigation of ^{240}Pu self-shielding effect at 1.056-eV and increase of ^{240}Pu capture reaction rate. The reactivity fluctuation over whole fuel burn-up also reduced from 30% to 6% in the design. Uncertainty evaluation in the initial reactivity based on nuclear data uncertainties in the JENDL4.0 library revealed that the proposed IMF design presented higher uncertainty of 1.8% relative to 1.3% for TRU oxide kernel at 0%FIMA due to higher nuclear data uncertainty in ^{240}Pu σ(n,γ). The initial reactivity in the proposed IMF design was enough high to keep its criticality at least at the beginning of the fuel cycle.

Acknowledgements

The authors would like to thank Director and Institute Professor M. Saito, Academy for Global Nuclear Safety and Security Agent, Tokyo Institute of Technology, for his encouragement and advice. The authors also express their gratitude to Dr. T. Yoshida, for continual support in preparation for publishing.

References

[1] C. Rodriguez, A. Baxter, D. McEachern, M. Fikani, F. Venneri and Deep-Burn: Making nuclear waste transmutation practical, *Nucl. Eng. Des.* 222 (2003), pp. 299-317.

[2] T. Aoki, H. Sagara and S. S. Chirayath, Proliferation Resistance Evaluation for TRU Fuel Cycle employing HTGR using PRAETOR code, *Annuls of Nuclear Energy* (to be submitted)

[3] K. C. Jo, Y. Kim, F. Venneri and M. J. Noh, Study on TRU Deep-Burn with a Silicon Carbide Inert Matrix Fuel in an MHR, *2009 ANS Winter Meeting*, Washington DC, USA, Nov. 15-19, (2009), [CD-ROM]

[4] T. Sakai, H. Sagara and M. Saito, Minimizing Burnup Reactivity of TRU Fuel by its Resonance Capture, *Proc. 2010 Fall Meeting of the At. Energy Soc. Jpn.*, Hokkaido, Japan, Sep. 15-17, (2010), [in Japanese] [CD-ROM].

[5] Y. Fukaya, M. Goto, H. Ohashi, Y. Tachibana, K. Kunitomi and S. Chiba, Proposal of a plutonium burner system based on HTGR with high proliferation resistance, *J. Nucl. Sci. Technol.* 51 (2014), pp. 818-831.

[6] Y. Nagaya, K. Okumura, T. Mori and M. Nakagawa, *MVP/GMVP II : General Purpose Monte Carlo Codes for Neutron and Photon Transport Calculations based on Continuous Energy and Multigroup Methods*, JAERI 1348, Japan Atomic Energy Research Institute, (2004).

[7] K. Shibata, O. Iwamoto, T. Nakagawa, et al., JENDL-4.0: a new library for nuclear science and engineering, *J. Nucl. Sci. Technol.* 48 (2011), pp. 1-30.

[8] I. Murata, A. Takahashi, T. Mori, et al., New sampling method on continuous energy Monte Carlo calculation for pebble bed reactors, *J. Nucl. Sci. Technol.* 24 (1997), pp. 734-744.

[9] K. Sawa and S. Yoshimuta, *Design of Coated Fuel Particle for High Burnup High Temperature Gas-cooled Reactor*, JAERI-Tech 98-025, Japan Atomic Energy Research Institute, (1998). [in Japanese].

[10] J.J. Duderstadt and L.J. Hamilton, *Nuclear Reactor Analysis*, John Wiley & Sons, New York, (1942), p. 344.